Journal of Molecular Graphics and Modelling 33 (2012) 19–25

Contents lists available at SciVerse ScienceDirect

Journal of Molecular Graphics and Modelling

journal homepage: www.elsevier.com/locate/JMGM

Theoretical investigations on electronic spectra and the redox-switchable second-order nonlinear optical responses of rhodium(I)-9,10-phenanthrenediimine complexes

Xiao-Juan Li, Shi-Ling Sun, Na-Na Ma, Xiu-Xin Sun, Guo-Chun Yang, Yong-Qing Qiu*

Institute of Functional Material Chemistry, Faculty of Chemistry, Northeast Normal University, Changchun 130024, People's Republic of China

ARTICLE INFO

Article history:
Received 24 July 2011
Received in revised form 4 November 2011
Accepted 7 November 2011
Available online 20 November 2011

Keywords:
Redox-switchable NLO property
DFT
Rh(I) complex
Charge-transfer

ABSTRACT

The redox-switchable second-order nonlinear optical (NLO) properties of a series of Rh(I) complexes have been studied based on density functional theory (DFT) calculations. The analysis of the electronic structure shows that the Rh(I) ion acts as the oxidation center in a one-electron-oxidized process, while both the Rh(I) ion and the 9,10-phenanthrenediimine (phdi) ligand act as reduction centers in a one-electron-reduced process. Different redox centers lead to different charge-transfer (CT) features, which alter the static first hyperpolarizabilities of the neutral complexes. Our DFT calculations indicated that these complexes show large second-order NLO responses and that the redox process can significantly enhance these NLO responses. For complexes **2** and **3**, the β_{tot} values of the one-electron-reduced species $\mathbf{2}^{-}$ and the one-electron-oxidized species $\mathbf{3}^{+}$ are ~10.0 and ~8.5 times larger, respectively, than those of the corresponding neutral complexes. Therefore, complexes **2** and **3** are promising candidates for redox-switchable NLO molecular materials. The large NLO responses of the oxidized species are mainly related to ligand-to-ligand charge-transfer (LLCT) transitions when combined with intraligand charge-transfer (ILCT) transitions, while the results for the reduced species are strongly associated with metal-to-ligand charge-transfer (MLCT) transitions.

1. Introduction

During the past two decades, molecular materials with nonlinear optical (NLO) properties have attracted considerable attention due to their potential applications in novel optoelectronic devices for telecommunications, information storage, optical switching and signal processing [1–4]. Recently, metal complexes with potential NLO properties have become the hotspot for research due to their good thermal photochemical stability and redox switching ability [5–7]. Compared with inorganic and organic materials, metal complexes possess low-lying charge-transfer (CT) states that can be associated with large NLO responses [8–11]. Among these studies, transition metal complexes represent an emerging and growing class of materials. For example, the second-order NLO properties of bis(salicylaldiminato)M^{II} (M = Co, Ni, Cu) Schiff base complexes have been reviewed by Di Bella et al. [11,12] and the results indicate that the central metal can significantly enhance the first hyperpolarizabilities. Moreover, a series of theoretical investigations [13,14] on the NLO properties of Ni, Pd and Pt complexes have been performed, and the results suggest that these complexes exhibit excellent NLO responses. Furthermore, in experimental and theoretical investigations, several effective methods have been developed to enhance the second-order NLO responses of the metal complexes, such as appropriate ligand selection, donor-π bridge-acceptor (D-π-A) structure formation [15,16], and metal n*d* configuration and spin state changes [17,18].

As is well known, the molecular second-order NLO properties depend not only on the nature of the π-conjugated bridge but also on the strength of the donor and acceptor groups. A reversible redox is a more appealing method for controlling the second-order NLO responses of a molecule because the oxidation/reduction process alters the capacity of the donor/acceptor [19,20]. For instance, Coe et al. [21–24] studied a series of ruthenium(II) complexes, and their results indicated that redox process with their metal ruthenium could significantly affect the first hyperpolarizabilities. Furthermore, the second-order NLO of metalloporphyrin complexes containing tetrathiafulvalene (TTF) were investigated by Liu et al. [25], and their results indicated that both TTF and the metal ion were oxidation centers and that the NLO responses were significantly increased by the oxidation process. Recently, a series of square-planar Rh(I) complexes (**2a** and **2b**) with the ligand 9,10-phenenthrenediimine (phdi) were prepared and electrochemically studied. Cyclic voltammetry of **2a** ([dpp-nacnac^{CH3}]Rh(I)(phdi); [dpp-nacnac^{CH3}]$^{-}$ = CH[C(Me)

* Corresponding author. Fax: +86 431 85098768.
E-mail address: qiuyq466@nenu.edu.cn (Y.-Q. Qiu).

1093-3263/$ – see front matter © 2011 Elsevier Inc. All rights reserved.
doi:10.1016/j.jmgm.2011.11.002

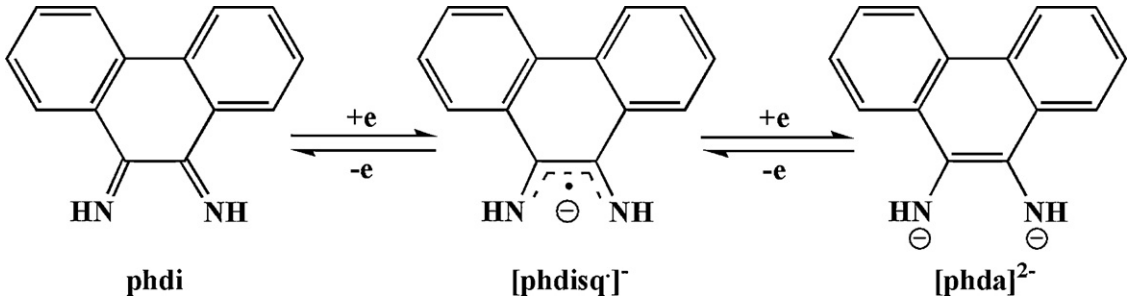

Scheme 1. Redox-active ligand of Phdi.

$(N\text{-}^{i}Pr_2C_6H_3)]_2^-$) showed that the reversible one-electron oxidation peak potential (E_p^{ox}) was 0.06 V vs. $[Cp_2Fe]^{+/0}$, and the reversible one-electron reduction potential (E^{red}) was −2.03 V vs. $[Cp_2Fe]^{+/0}$ [26]. This electrochemical study indicated that both the phdi ligand and the Rh(I) metal were redox-active. Notably, the ligand phdi is a closed-shell neutral ligand, where a one-electron reduction affords an open-shell diiminosemiquinonate ($[phdisq^{\bullet}]^-$), and a two-electron reduction affords a closed-shell phenanthrenediamide form ($[phda]^{2-}$), as shown in Scheme 1. Accordingly, the redox properties of the diimine moiety can affect the delocalization of the frontier molecular orbitals, which can cause changes in its NLO properties. Thus, an ideal model for the redox switching of the NLO responses was provided.

Quantum chemical calculations are quite helpful when synthesizing and testing NLO materials. In addition, density functional theory (DFT) has been shown to be extremely useful in treating the electronic structures and in predicting their linear and nonlinear optical properties [27,28]. In this article, we have investigated the redox-switchable second-order NLO responses of Rh(I) complexes containing $-CH_3$ and $-CF_3$ groups and having redox behaviors based on the DFT. We also designed two other Rh(I) complexes that contained either a strong electron donor ($-NH_2$) or a strong electron acceptor ($-NO_2$) in place of the $-CH_3$ or $-CF_3$ of the above Rh(I) complexes (see Fig. 1); their redox-switchable second-order NLO responses were also calculated. Meanwhile, the details of the electron spectra were revealed by the time-dependent density functional theory (TD-DFT).

2. Computational details

All calculations were performed by the Gaussian 09W program package [29]. The geometries of all of the complexes were optimized at the (U)PBE1PBE/6-31G* level. The PBE1PBE, also known as PBE0, is obtained by casting the functional and correlation of Perdew, Burke and Erzenrhof in a hybrid Hartree-Fock (HF)/DFT scheme with a fixed 1/4 ratio [30,31]. Considering the relativistic effects for the transition metal ions, SDD basis set containing the Stuttgart–Dresden effective core potentials was applied for the Rh(I) ion. It is known that TD-DFT is one of the most popular methods for calculating electron absorption spectra in quantum chemistry [32,33] because the accuracy and reliability of the spin-unrestricted TD-DFT for open-shelled systems have been tested, studying both organic and transition metal complexes [34–39]. Thus, TD-DFT was adopted in this work to calculate the electron spectra of the studied systems. Moreover, we used polarized continuum model (PCM) at the same level to calculate the absorption spectra [40,41].

The finite field (FF) method was broadly applied because this methodology can be used in concert with the electron structure method to compute the static first hyperpolarizabilities (β) [42,43]. Based on the optimized geometries, in this article, we studied the static first hyperpolarizabilities (β) of all of the complexes using the FF method with a field frequency of 0.0010 a.u. by long range-corrected (LC) functional LC-ωPBE, the 6-31g* basis set was employed for nonmetal atoms and the SDD basis set for the Rh(I) ion. Recently, the LC-ωPBE functional was reported as a successful method for computing the first hyperpolarizabilities [44,45]. Therefore, the static first hyperpolarizabilities (β_{tot}) for all of the complexes were calculated using the following formula:

$$\beta_{tot} = \sqrt{\beta_x^2 + \beta_y^2 + \beta_z^2} \quad (1)$$

where β_i is defined by the following equation (Eq. (2)):

$$\beta_i = \beta_{iii} + \frac{1}{3}\sum_{i \neq j}[(\beta_{ijj} + \beta_{jij} + \beta_{jji})], \quad i, j = x, y, z \quad (2)$$

3. Results and discussion

3.1. Molecular structure

To save on computational costs, complexes **1** and **2** were obtained by replacing the isopropyl groups on the benzenes of **2a** and **2b** with hydrogen atoms (Fig. 1). All of these complexes had C_s symmetry; therefore, the origins of the Cartesian coordinate systems for each was located at the Rh(I). Furthermore, the *y*-axis pointed to the nacnac ligand, and the *yz* plane was in the plane of the molecule. The coordination bond lengths of complexes **1**, **2**, **3** and **4** and the experimental data of complex **1** are reported in Table 1. From Table 1, the calculated Rh-N1 bond length of complex **1** was only 0.0031 Å longer than the reported crystallographic data, while the Rh-N2 bond length was 0.0049 Å shorter; these results indicated that the method and the basis sets selected were reliable. The bond lengths of complexes **2**, **3**, and **4** did not significantly change compared with **1**. However, the coordination bond lengths of the redox species changed noticeably. For example, the value of the Rh-N2 bond of the species $\mathbf{1}^+$ increased to 2.0348 Å, while that of the Rh-N1 bond of species $\mathbf{1}^-$ reached up to 2.0403 Å. Based on the performed spin-unrestricted calculations, the spin contaminations $\langle S^2 \rangle$ of $\mathbf{1}^+$, $\mathbf{1}^-$, $\mathbf{2}^+$, $\mathbf{2}^-$, $\mathbf{3}^+$, $\mathbf{3}^-$, $\mathbf{4}^+$ and $\mathbf{4}^-$ were found to be 0.758, 0.761, 0.756, 0.766, 0.808, 0.760, 0.755 and 0.776, respectively, which were quite close to the theoretical values ($S^2 = 0.75$).

Table 1
The coordination bond lengths (Å) of complexes by (U)PBE1PBE/6-31G*.

Complexes	Lengths	
	Rh-N1	Rh-N2
1	2.0128 (2.0097)	1.9783 (1.9832)
2	2.0105	1.9831
3	2.0283	1.9708
4	2.0209	1.9768
$\mathbf{1}^+$	2.0136	2.0348
$\mathbf{1}^-$	2.0403	1.9933

The data in parentheses are the crystal structure data of complex **1**.

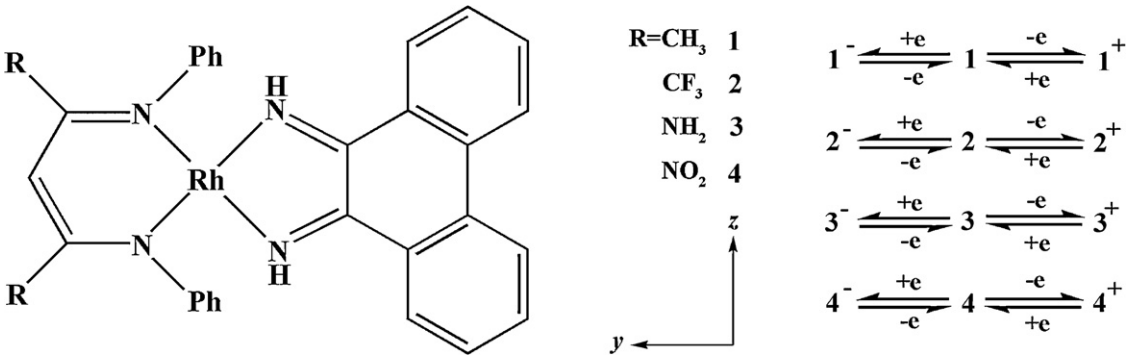

Fig. 1. The calculation models of all of the complexes.

Overall, these findings indicated that spin contamination was negligible.

3.2. Electronic spectra properties

The absorption spectra of complexes **2a** and **2b** ([dpp-nacnac^{CF3}]Rh(I)(phdi)) have been measured using experiment [26] in CH_2Cl_2. Both showed two intense absorption bands in the UV–vis region: 362 nm and 593 nm for **2a** and 312 nm and 587 nm for **2b**. The PBE1PBE functional has been demonstrated to improve the accuracy of excitation energies and charge-transfer bands in organic metal complexes for both gas phase and solution calculations [46,47]. Thus, the TD-PBE1PBE/6-31G* level (the SDD basis set for the Rh ion) was selected to simulate the absorption spectra of **2a** and **2b** in CH_2Cl_2 solution using the PCM. For the TD-DFT calculations, two intense absorption bands at 316.2 nm and 566.3 nm for **2a** and two intense CT transitions at 277.2 nm and 540.3 nm for **2b** were found. It can be seen that the simulated absorption bands are similar to those of the experiments, although blue shifts of approximately 27–47 nm were also observed, which could be ascribed to the deficiency in flexibility that the TD-DFT method has in describing states with CT.

Consequently, we calculated the absorption spectra of all of the complexes at the PBE1PBE level. The TD-DFT calculated excited energy (E_{gm}), absorption wavelengths (λ), oscillator strengths (f_{os}) and associated orbital transitions are listed in Table 2. The results show that complex **1** has two intense absorption bands at 560.8 nm and 314.0 nm, while complex **2** has bands at 536.2 nm and 272.3 nm. These data Exhibit 24.6 nm and 41.7 nm blue shifts in the low- and high-energy bands caused by replacing $-CH_3$ with $-CF_3$. Complexes **3** and **4** also have two absorption bands for their low- and high-energy bands. In addition, similar absorption spectra are observed in the oxidized species $\mathbf{1}^+$, $\mathbf{2}^+$, $\mathbf{3}^+$ and $\mathbf{4}^+$ and the reduced species $\mathbf{1}^-$, $\mathbf{2}^-$ and $\mathbf{3}^-$. Interestingly, only species $\mathbf{4}^-$ shows an intense absorption band at 711.3 nm. When comparing the oxidized/reduced species with their corresponding neutral complexes, the redox process induces a substantial red shift in the absorption bands of the oxidized/reduced species. For instance, in the case of $\mathbf{1}^+$ and $\mathbf{2}^+$, red shifts of 85.1 nm and 33.4 nm, respectively, in the low-energy absorption band of each are observed, whereas the largest red shift of 176.1 nm is observed with complex $\mathbf{2}^-$ and a red shift of 140.7 nm is induced in complex $\mathbf{1}^-$.

The absorption spectra of series **2** are essentially similar to those of series **1**. Therefore, series **1** was used to investigate the CT caused by the redox reaction; the corresponding molecular orbital (MOs) transitions of each complex, **1**, $\mathbf{1}^+$ and $\mathbf{1}^-$, are listed in Fig. 2. From the calculations for complex **1**, the low-energy absorption (560.8 nm) was attributed to the HOMO→LUMO transition, which can be described as the nacnac to phdi ligand charge-transfer (LLCT). Furthermore, the high-energy absorption at 314.0 nm was related to the HOMO-1→LUMO+2 transition because of the metal-to-ligand charge-transfer (MLCT). Therefore, these results indicated that the nacnac ligand and Rh metal act as electron donor, while the phdi ligand acts as the electron acceptor. For the oxidized species $\mathbf{1}^+$, the αHOMO and βHOMO are predominantly localized on the nacnac ligand, the αLUMO is mainly localized on phdi ligand, and the βLUMO is largely localized on the Rh metal. Therefore, the low-energy absorption at 645.9 nm for $\mathbf{1}^+$ represents the αHOMO→αLUMO and βHOMO→βLUMO transitions, which possess LLCT and LMCT (ligand-to-metal charge-transfer from the nacnac ligand to the Rh ion) characters. Moreover, the αHOMO→αLUMO+4 and βHOMO→βLUMO+4 transitions involved in the high-energy absorption (301.0 nm) are contributed to the $\pi\rightarrow\pi^*$ intraligand charge-transfer (ILCT). Thus, changes in the CT that are induced by oxidation may have important effects on the static first hyperpolarizabilities. Moreover, the TD-DFT calculations show that the low-energy absorption of the one-electron-reduced species $\mathbf{1}^-$ contributed by the βHOMO→βLUMO transition can be described as a weak MLCT transition. Furthermore, the high-energy absorption at 347.4 nm containing the αHOMO-1→αLUMO+1 and βHOMO-1→βLUMO+2 transitions is likely caused by the αHOMO-1 being totally delocalized on the Rh metal, while the βHOMO-1 is delocalized on the whole molecule. However, the electron densities of the αLUMO+1 and βLUMO+2 are located on both the nacnac and phdi ligands, thus generating a strong CT from the Rh ion to the ligand (MLCT). Obviously, the Rh ion acts as an electron donor in the CT process, which may alter the second-order NLO responses. Interestingly, similar phenomena were observed in the other complexes except for species $\mathbf{3}^+$ and $\mathbf{4}^+$, whose high-energy absorption CTs were LLCTs.

3.3. Second-order NLO properties

β is a third-rank tensor described by a $3\times3\times3$ matrix. In this static limit, β is symmetric in all of the indices; therefore, we could reduce the 27 components matrix to a 10 components matrix based on Kleinman symmetry [48]. The 10 components of the first hyperpolarizabilities for all of the complexes were calculated by using the FF method. The static first hyperpolarizabilities (β_{tot}) for all of the complexes were calculated by using Eq. (1). In this article, we studied the second-order NLO responses of all of the complexes by LC-ωPBE functional.

3.3.1. The first hyperpolarizabilities of neutral complexes

The β_{xxz}, β_{yyz} and β_{zzz} tensor components and the β_{tot} values for all of the complexes are shown in Table 3, and the β_{tot} value of complex **1** is ~2.1 times as large as that of complex **2**. The reason this change occurred is that the $-CH_3$ group is a weak electron-donating unit, while the $-CF_3$ unit has a weak electron-withdrawing ability.

Table 2
Excitation energy (λ, nm; E_{gm}, eV), oscillator strengths (f_{os}), and corresponding dominant MO transitions complexes.

Complexes	λ/nm	E_{gm}/eV	f_{os}	Major contributions	Assignment
1	560.8	2.21	0.5161	HOMO→LUMO (99%)	LLCT
	314.0	3.95	0.4590	HOMO-1→LUMO+2 (88%)	MLCT
2	536.2	2.31	0.5288	HOMO→LUMO (99%)	LLCT
	299.8	4.14	0.1354	HOMO-2→LUMO+2 (65%)	MLCT
3	584.4	2.12	0.4107	HOMO→LUMO (98%)	LLCT
	326.5	3.80	0.3523	HOMO-1→LUMO+2 (88%)	MLCT
4	525.2	2.36	0.5887	HOMO→LUMO (97%)	LLCT
	291.0	4.26	0.1643	HOMO-3→LUMO+2 (24%)	LLCT
				HOMO→LUMO+5 (22%)	MLCT
1^{+}	645.9	1.92	0.3188	αHOMO→αLUMO (56%)	LLCT
				βHOMO→βLUMO (44%)	LMCT
	301.0	4.12	0.1415	αHOMO→αLUMO+4 (28%)	ILCT
				βHOMO→βLUMO+4 (20%)	ILCT
2^{+}	569.6	2.18	0.2980	αHOMO→αLUMO (58%)	LLCT
				βHOMO→βLUMO (42%)	LLCT
	346.3	3.58	0.1909	αHOMO→αLUMO+1 (31%)	ILCT
				βHOMO→βLUMO+2 (31%)	ILCT
3^{+}	658.6	1.88	0.1965	αHOMO→αLUMO (52%)	LLCT
				βHOMO→βLUMO+1 (42%)	LLCT
	493.5	2.51	0.1673	βHOMO-3→βLUMO (83%)	LLCT
4^{+}	534.9	2.32	0.3254	αHOMO→αLUMO (58%)	LLCT
				βHOMO→βLUMO (41%)	LLCT
	360.0	3.44	0.1094	βHOMO-7→βLUMO (48%)	LLCT
				αHOMO-7→αLUMO (31%)	LLCT
1^{-}	701.5	1.77	0.2092	βHOMO→βLUMO (93%)	MLCT
	347.4	3.57	0.3222	αHOMO-1→αLUMO+1 (58%)	MLCT
				βHOMO-1→βLUMO+2 (21%)	MLCT
2^{-}	712.3	1.74	0.2359	βHOMO→βLUMO (90%)	MLCT
	347.3	3.57	0.0989	βHOMO-5→βLUMO (51%)	LLCT
				βHOMO-1→βLUMO+3 (14%)	MLCT/LLCT
3^{-}	684.8	1.81	0.1293	βHOMO→βLUMO (83%)	MLCT
	347.8	3.56	0.1986	αHOMO-1→αLUMO+1 (17%)	MLCT
				βHOMO→βLUMO+4 (15%)	MLCT/LLCT
4^{-}	711.3	1.74	0.3375	βHOMO→βLUMO+2 (54%)	MLCT/LLCT
				βHOMO→βLUMO+1 (36%)	MLCT

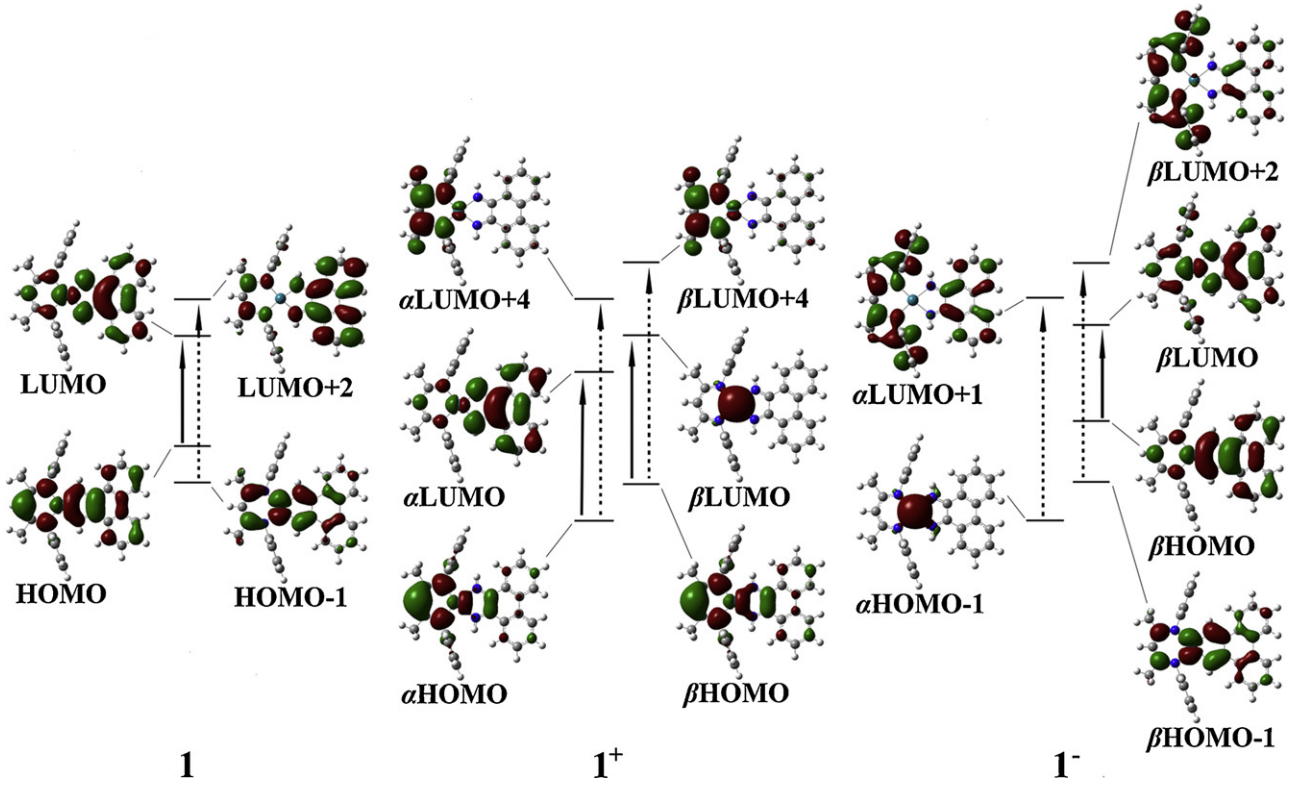

Fig. 2. The molecular orbital transitions of complexes **1**, **1**$^{+}$ and **1**$^{-}$ (the solid arrows represent low-energy transitions and the dashed arrows represent high-energy transitions).

Table 3
The first hyperpolarizabilities (1×10^{-30} esu) obtained by (U)LC-ωPBE method.

Complexes	β_{yyy}	β_{yzz}	β_{xxy}	β_{tot}
1	−18.933	−6.804	1.995	23.742
2	−7.142	−5.824	1.448	11.517
3	−21.455	−11.533	2.006	30.982
4	−3.755	−6.067	1.278	8.544
$\mathbf{1}^+$	−43.294	−3.936	−0.428	47.658
$\mathbf{2}^+$	−69.123	−6.409	11.853	66.846
$\mathbf{3}^+$	−248.758	−14.101	0.899	261.960
$\mathbf{4}^+$	−38.234	−14.027	0.532	51.729
$\mathbf{1}^-$	132.919	−13.517	2.214	121.663
$\mathbf{2}^-$	127.847	−15.078	2.688	115.457
$\mathbf{3}^-$	75.966	−18.583	4.562	61.946
$\mathbf{4}^-$	57.583	−9.565	1.898	49.918

Therefore, according to the TD-DFT calculation results mentioned above, the nacnac ligand acting as an electron donor, while the $-CF_3$ unit maybe decreasing the donor capacity of the nacnac ligand; these effects would cause a smaller second-order NLO coefficient for **2** to be achieved. For the β_{tot} value of complex **3**, an increase of $\sim 31 \times 10^{-30}$ esu occurs when the $-CH_3$ group is replaced by a strong electron-donating unit $-NH_2$, while the $-NO_2$ substituted complex **4** had a smaller static first hyperpolarizability. DFT-FF calculations show that the static first hyperpolarizabilities increased in the following order: $\beta_{tot(\mathbf{4})} < \beta_{tot(\mathbf{2})} < \beta_{tot(\mathbf{1})} < \beta_{tot(\mathbf{3})}$; these results indicate that the changes in the substituent group ($-CH_3$, $-NH_2$, $-CF_3$ and $-NO_2$) affected the second-order NLO responses for the series of Rh(I) complexes. Furthermore, the $-NH_2$ substituted **3** displayed a desirable NLO property, which was ~1.3, ~2.7 and ~3.6 times as large as the NLO properties of complexes **1**, **2** and **4**, respectively. Therefore, complex **3** could pose as an excellent NLO molecular material. The absorption spectra of **3** and **4** are essentially similar to that of complexes **1** and **2** (Table 2); the low-energy absorption for these complexes was pure HOMO→LUMO transition, which can be assigned to the CT from the nacnac ligand to the phdi ligand, while the high-energy absorption can be contributed to metal-to-ligand charge transfer. Overall, the second-order NLO responses of these complexes are mainly related to LLCT and MLCT transitions. Moreover, the molecular hyperpolarizabilities of a series of M(diimine) complexes (M = Pt, pd, Ni) have been obtained from electric field induced second harmonic generation (EFISHG) experiments at 1.9 μm and the range in magnitude is from 0 to -39×10^{-30} esu [49], and theoretical values of our studied complexes **1**–**4** were basically in the range of 8 to 31×10^{-30} esu. It indicated that the first hyperpolarizabilities of our studied complexes were consistent with the experimental data.

3.3.2. *Redox-switchable of NLO responses*

In the present paper, phdi is a redox-active ligand used to coordinate redox-active metal ions. Therefore, the one-electron-oxidized and one-electron-reduced of these four complexes (**1**, **2**, **3** and **4**) could occur in different locations, and the assignments of the oxidation and reduction centers in these complexes are particularly important. For this study, the redox centers of complexes **1**, **2**, **3** and **4** were first determined by analyzing the spin densities. From Fig. 3, the spin densities of the oxidized species ($\mathbf{1}^+$, $\mathbf{2}^+$, $\mathbf{3}^+$ and $\mathbf{4}^+$) were mainly localized on the Rh ions, which indicate that the Rh ions are the oxidation centers for each of the one-electron-oxidized processes. For the one-electron-reduced species ($\mathbf{1}^-$, $\mathbf{2}^-$, $\mathbf{3}^-$ and $\mathbf{4}^-$), except the Rh ion, the spin densities were also localized on the phdi ligand, which indicates that the Rh ion and the phdi ligand act as the reduction centers. Overall, these results may alter the CT features of the redox species relative to their neutral species, and thus, the second-order NLO properties of **1**, **2**, **3** and **4** might be improved.

According to the TD-DFT results, the CT of the neutral complexes (**1**, **2**, **3** and **4**) and the one-electron-oxidized species ($\mathbf{1}^+$, $\mathbf{2}^+$, $\mathbf{3}^+$ and $\mathbf{4}^+$) were mainly related to the LLCT transitions (from the nacnac ligand to the phdi ligand charge-transfers). Although the nacnac lig-

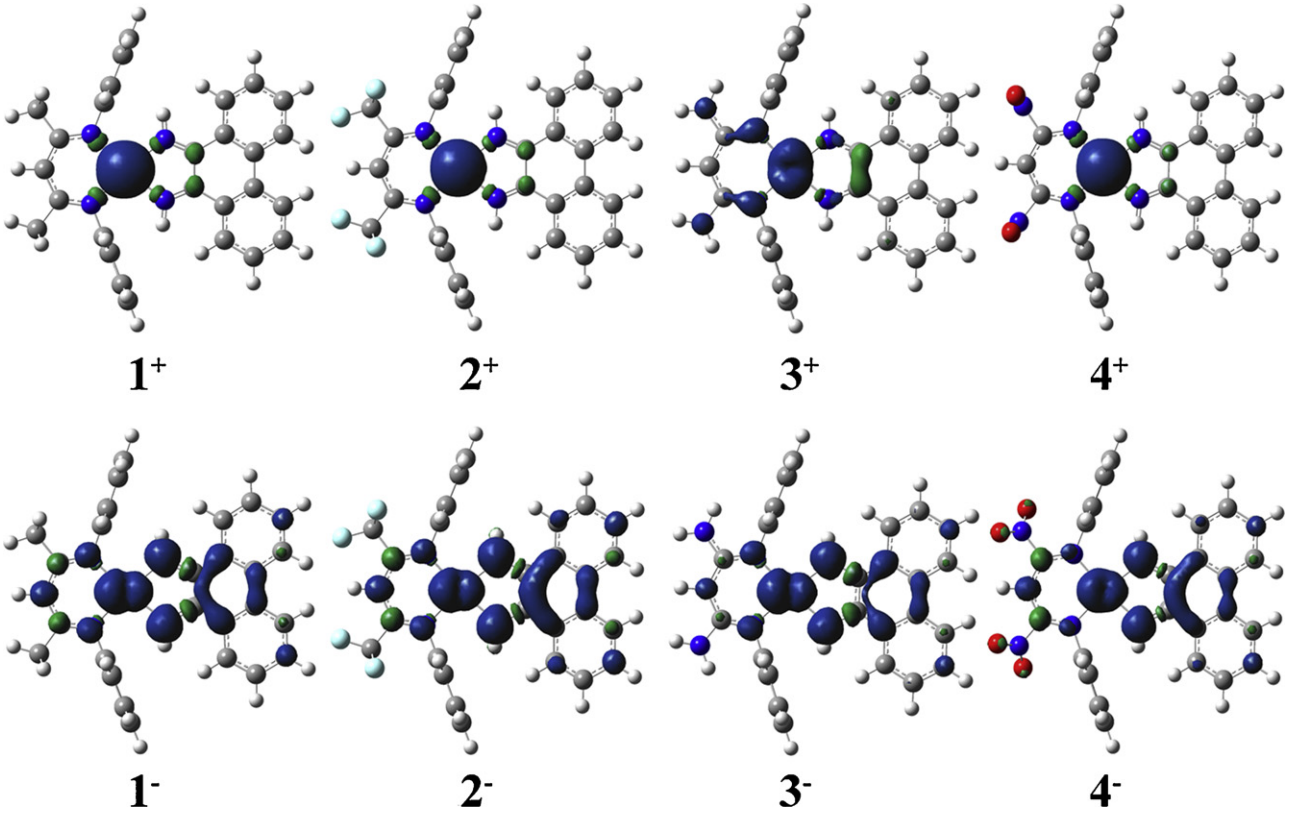

Fig. 3. The spin density plots of oxidized species and reduced species obtained by UPBE1PBE/6-31G* (SDD basis set on Rh ion).

and acts as electron donor in the neutral complexes and oxidized species, the donor capacities in the oxidized species are stronger than those of the neutral complexes (Fig. 2); thus, the second-order NLO properties of the oxidized species may be enhanced. According to our DFT-FF calculations, the β_{tot} values of the one-electron-oxidized species $\mathbf{1}^+$, $\mathbf{2}^+$, $\mathbf{3}^+$ and $\mathbf{4}^+$ are larger than those of the corresponding neutral complexes. For instance, the β_{tot} of $\mathbf{3}^+$ is ~8.5 times as large as that of the neutral complex **3**. Therefore, the $-NH_2$ substituted **3** could become an excellent redox-switchable NLO molecular material, Moreover, the second-order NLO properties of the reduced species $\mathbf{1}^-$, $\mathbf{2}^-$, $\mathbf{3}^-$ and $\mathbf{4}^-$, they were also enhanced compared with the corresponding neutral complexes. These results indicate that adding one electron causes a substantial enhancement in the molecular second-order NLO response. In particular, the β_{tot} value of $\mathbf{2}^-$ is ~10.0 times as large as that of complex **2**. Therefore, the complex **2** may be promising to become a potential redox-switchable NLO molecular material. Based on previous studies, the second-order NLO responses of the species $\mathbf{1}^-$, $\mathbf{2}^-$, $\mathbf{3}^-$ and $\mathbf{4}^-$ can be strong due to the MLCT transitions. Overall, those indicate that removing or adding one electron could cause substantial enhancement in the molecular second-order NLO responses.

Based on the complex sum-over-states expression, Oudar and Chemla established a simple link between the molecular first hyperpolarizabilities and CT transition through a two-level model [50,51]:

$$\beta \propto \frac{\Delta\mu_{gm} f_{os}}{\Delta E_{gm}^3} \quad (4)$$

where $\Delta\mu_{gm}$ is the difference between the dipole moments of the ground state (g) and the mth excited state (m), f_{os} is the oscillator strength, and E_{gm} is the transition energy. The first hyperpolarizability is proportional to the oscillator strength and inversely proportional to the cube of the transition energy. Therefore, a low transition energy is a main factor for achieving a large β value. In Table 2, the transition energies of the neutral complexes in the low-energy absorption bands are as follows: $E_{gm(\mathbf{4})} > E_{gm(\mathbf{2})} > E_{gm(\mathbf{1})} > E_{gm(\mathbf{3})}$. However, a smaller transition energy could significantly enhance the β_{tot} value. Thus, the computed β_{tot} values of the neutral complexes are as follows: $\beta_{tot(\mathbf{3})} > \beta_{tot(\mathbf{1})} > \beta_{tot(\mathbf{2})} > \beta_{tot(\mathbf{4})}$. For the redox species, substantial red shifts of the low-energy absorption bands are induced by redox; therefore, the transition energies of the redox species are reduced. For instance, in the cases of **1** and **2**, the transition energies of species $\mathbf{1}^+$ (1.92 eV) and $\mathbf{1}^-$ (1.77 eV) are smaller than that of complex **1** (2.21 eV). Additionally, the transition energies for species $\mathbf{2}^+$ (2.18 eV) and $\mathbf{2}^-$ (1.74 eV) are smaller than that of the complex **2** (2.31 eV) in the low-energy absorption band, which means that the second-order NLO properties for the redox species are significantly enhanced. Furthermore, the obvious differences on the first hyperpolarizabilities between the $-CH_3$ and $-NH_2$ substituted oxidized species $\mathbf{1}^+$ and $\mathbf{3}^+$ were observed. (β_{tot} value of $\mathbf{3}^+$ is ~5.5 times as large as that of species $\mathbf{1}^+$). A careful analysis of Table 2 shows that their high-energy transition is significantly different, and the transition energy of species $\mathbf{3}^+$ (2.51 eV) is smaller than that of the species $\mathbf{1}^+$ (4.12 eV), and thus $\mathbf{3}^+$ shows larger β_{tot}. For the reduced species $\mathbf{2}^-$ and $\mathbf{4}^-$, the species $\mathbf{2}^-$ has two intense absorption bands while the species $\mathbf{4}^-$ only shows an intense absorption band at 711.3 nm, which perhaps cause that the β_{tot} value of $\mathbf{2}^-$ is ~2.3 times as large as that of species $\mathbf{4}^-$.

4. Conclusions

Systematic DFT calculations were performed on square-planar Rh(I) complexes with redox-active ligands, and the electron absorption spectra for all of the complexes in the UV–vis region were investigated by the TD-DFT approach combined with PCM solvent model. Our DFT-FF calculations indicated that the substituent groups ($-CH_3$, $-NH_2$, $-CF_3$ and $-NO_2$) had some effects on the NLO responses of these complexes, and the $-NH_2$ substituted **3** complex displayed the most desirable NLO properties. For the redox-switchable second-order NLO responses of the complexes **1**, **2**, **3** and **4**, it was found that removing or adding one electron could reduce the transition energy and change the CT feature, therefore, the static first hyperpolarizabilities were enhanced. With complexes **2** and **3**, the β_{tot} values of the one-electron-reduced species $\mathbf{2}^-$ and the one-electron-oxidized species $\mathbf{3}^+$ were ~10.0 and ~8.5 times as large as those for their corresponding neutral complexes, respectively. Therefore, the complexes **2** and **3** were promising to become novel redox-switchable NLO molecular materials. The large NLO responses of the oxidized species were mainly related to the LLCT transitions combined with ILCT transitions, and the reduced species were strongly assigned to the MLCT transitions. In summation, the studied Rh(I) metal complexes are promising candidates for redox-switchable second-order NLO materials.

Acknowledgments

The authors gratefully acknowledge the financial support provided by the National Natural Science Foundation of China (No. 20873017) and the Natural Science Foundation of Jilin province (20101154).

References

[1] J.P. Costes, J.F. Lamère, C. Lepetit, P.G. Lacroix, F. Dahan, Synthesis, crystal structures, and nonlinear optical (NLO) properties of new Schiff-base nickel(II) complexes. Toward a new type of molecular switch? Inorg. Chem. 44 (2005) 1973–1982.
[2] X. Zhou, Q.J. Pan, B.H. Xia, M.X. Li, H.X. Zhang, A.C. Tung, DFT and TD-DFT calculations on the electronic structures and spectroscopic properties of cyclometalated platinum(II) complexes, J. Phys. Chem. A 111 (2007) 5465–5472.
[3] S. Di Bella, I. Fragalà, Synthesis and second-order nonlinear optical properties of bis(salicylaldiminato)M(II) metalloorganic materials, Synth. Met. 115 (2000) 191–196.
[4] P.G. Lacroix, Second-order optical nonlinearities in coordination chemistry: the case of bis(salicylaldiminato)metal Schiff base complexes, Eur. J. Inorg. Chem. (2001) 339–348.
[5] F. Tessore, D. Locatelli, S. Righetto, D. Roberto, R. Ugo, An investigation on the role of the nature of sulfonate ancillary ligands on the strength and concentration dependence of the second-order NLO responses in $CHCl_3$ of Zn(II) complexes with 4,4′-trans-$NC_5H_4CH{=}CHC_6H_4NMe_2$ and 4,4′-trans,trans-$NC_5H_4(CH{=}CH)_2C_6H_4NMe_2$, Inorg. Chem. 44 (2005) 2437–2442.
[6] M. Malaun, Z.R. Reeves, R.L. Paul, J.C. Jeffery, J.A. McCleverty, M.D. Ward, I. Asselberghs, K. Clays, A. Persoons, Reversible switching of the first hyperpolarisability of an NLO-active donor–acceptor molecule based on redox interconversion of the octamethylferrocene donor unit, Chem. Commun. 1 (2001) 49–50.
[7] F. De Angelis, S. Fantacci, A. Sgamelotti, F. Cariati, D. Roberto, F. Tessore, R. Ugo, A time-dependent density functional theory investigation on the nature of the electronic transitions involved in the nonlinear optical response of [Ru(CF_3CO_2)$_3$T] (T = 4′-(C_6H_4-*p*-NBu_2)-2,2′:6′,2″-terpyridine), Dalton Trans. (2006) 852–859.
[8] S. Barlow, H.E. Bunting, C. Ringham, J.C. Green, G.U. Bublitz, S.G. Boxer, J.W. Perry, S.R. Marder, Studies of the electronic structure of metallocene-based second-order nonlinear optical dyes, J. Am. Chem. Soc. 121 (1999) 3715–3723.
[9] B.J. Coe, S.P. Foxon, E.C. Harper, J. Raftery, R. Shaw, C.A. Swanson, I. Asselberghs, K. Clays, B.S. Brunschwig, A.G. Fitch, Nonlinear optical and related properties of iron(II) pentacyanide complexes with quaternary nitrogen electron acceptor units, Inorg. Chem. 48 (2009) 1370–1379.
[10] B.J. Coe, J.A. Harris, B.S. Brunschwig, I. Asselberghs, K. Clays, J. Garín, J. Orduna, Three-dimensional nonlinear optical chromophores based on metal-to-ligand charge-transfer from ruthenium(II) or iron(II) centers, J. Am. Chem. Soc. 127 (2005) 13399–13410.
[11] S. Di Bella, I. Fragalà, I. Ledoux, T.J. Marks, Role of metal electronic properties in tuning the second-order nonlinear optical response of coordination complexes. A combined experimental and theoretical investigation of a homologous series of (N,N′-disalicylidene-1,2-phenylenediaminato)M(II) (M = Co Ni, Cu) complexes, J. Am. Chem. Soc. 117 (1995) 9481–9485.
[12] S. Di Bella, I. Fragalà, I. Ledoux, M.A. Diaz-Garcia, T.J. Marks, Synthesis, characterization, optical spectroscopic electronic structure, and second-order nonlinear optical (NLO) properties of a novel class of donor–acceptor

bis(salicylaldiminato) nickel(II) Schiff base NLO chromophores, J. Am. Chem. Soc. 119 (1997) 9550–9557.
[13] C.G. Liu, Y.Q. Qiu, S.L. Sun, H. Chen, N. Li, Z.M. Su, DFT study on second-order nonlinear optical properties of a series of mono Schiff-base M(II) (M = Ni, Pd Pt) complexes, Chem. Phys. Lett. 429 (2006) 570–574.
[14] P. Romaniello, M.C. D'Andria, F. Lelj, Nonlinear optical properties of Ni(Me_6pzS_2)MX (M = Ni, Pd Pt; X = Me_2timdt, mnt), J. Phys. Chem. A 11 (2010) 5838–5845.
[15] P. Hrobárik, I. Sigmundová, P. Zahradník, P. Kasák, V. Arion, E. Franz, K. Clays, Molecular engineering of benzothiazolium salts with large quadratic hyperpolarizabilities: can auxiliary electron-withdrawing groups enhance nonlinear optical responses? J. Phys. Chem. C 114 (2010) 22289–22302.
[16] S. Das, A. Nag, D. Goswami, P.K. Bharadwaj, Zinc(II)- and copper(I)-mediated large two-photon absorption cross sections in a bis-cinnamaldiminato Schiff base, J. Am. Chem. Soc. 128 (2006) 402–403.
[17] A. Baccouche, B. Peigné, F. Ibersiene, D. Hammoutène, A. Boutarfäa, A. Boucekkine, C. Feuvrie, O. Maury, I. Ledoux, H. Le Bozec, Effects of the metal center and substituting groups on the linear and nonlinear optical properties of substituted styryl-bipyridine metal(II) dichloride complexes: DFT and TD-DFT computational investigations and harmonic light scattering measurements, J. Phys. Chem. A 114 (2010) 5429–5438.
[18] H.B. Zhao, S.L. Sun, Y.Q. Qiu, C.G. Liu, Z.M. Su, Theoretical study on second-order nonlinear optical properties of spin crossover Fe(III) phenolate-pyridyl Schiff base complexes, Int. J. Quantum Chem. 110 (2010) 1863–1870.
[19] E. Hendrickx, K. Clays, A. Persoons, C. Dehu, J.L. Brédas, The bacteriorhodopsin chromophore retinal and derivatives: An experimental and theoretical investigation of the second-order optical properties, J. Am. Chem. Soc. 117 (1995) 3547–3555.
[20] R. Loucif-Saïbi, K. Nakatani, J.A. Delaire, M. Dumont, Z. Sekkat, Photoisomerization and second harmonic generation in disperse red one-doped and -functionalized poly(methyl methacrylate) films, Chem. Mater. 5 (1993) 229–236.
[21] B.J. Coe, J.A. Harris, L.J. Harrington, J.C. Jeffery, L.H. Rees, S. Houbrechts, A. Persoons, Enhancement of molecular quadratic hyperpolarizabilities in ruthenium(II) 4,4′-bipyridinium complexes by N-phenylation, Inorg. Chem. 37 (1998) 3391–3399.
[22] B.J. Coe, J.A. Harris, B.S. Brunschwig, Electroabsorption spectroscopic studies of dipolar ruthenium(II) complexes possessing large quadratic nonlinear optical responses, J. Phys. Chem. A 106 (2002) 897–905.
[23] B.J. Coe, L.A. Jones, J.A. Harris, B.S. Brunschwig, I. Asselberghs, K. Clays, A. Persoons, J. Garín, J. Orduna, Syntheses and spectroscopic and quadratic nonlinear optical properties of extended dipolar complexes with ruthenium(II) ammine electron donor and N-methylpyridinium acceptor groups, J. Am. Chem. Soc. 126 (2004) 3880–3891.
[24] B.J. Coe, Switchable nonlinear optical metallochromophores with pyridinium electron acceptor groups, Acc. Chem. Res. 39 (2006) 383–393.
[25] C.G. Liu, W. Guan, P. Song, L.K. Yan, Z.M. Su, Redox-switchable second-order nonlinear optical responses of push-pull monotetrathiafulvalene-metalloporphyrins, Inorg. Chem. 48 (2009) 6548–6554.
[26] D.W. Shaffer, S.A. Ryken, R.A. Zarkesh, A.F. Heyduk, Redox behavior of rhodium 9,10-phenanthrenediimine complexes, Inorg. Chem. 50 (2011) 13–21.
[27] T. Liu, H.X. Zhang, X. Zhou, Q.C. Zheng, B.H. Xia, Q.J. Pan, Mechanism of Ir($ppy)_2$(NÑ)$^+$ (NÑ = 2-phenyl-1*H*-imidazo[4 5-f][1,10]phenanthroline) sensor for F^-, CF_3COOH, and CH_3COO^-: density functional theory and time-dependent density functional theory studies, J. Phys. Chem. A 112 (2008) 8254–8262.
[28] C.G. Liu, Y.Q. Qiu, S.L. Sun, N. Li, G.C. Yang, Z.M. Su, DFT studies on second-order nonlinear optical properties of mono (salicylaldiminato) nickel(II) polyenyl Schiff base metal complexes, Chem. Phys. Lett. 443 (2007) 163–168.
[29] M.J. Frisch, G.W. Trucks, H.B. Schlegel, G.E. Scuseria, M.A. Robb, J.R. Cheeseman, G. Scalmani, V. Barone, B. Mennucci, G.A. Petersson, H. Nakatsuji, M. Caricato, X. Li, H.P. Hratchian, A.F. Izmaylov, J. Bloino, G. Zheng, J.L. Sonnenberg, M. Hada, M. Ehara, K. Toyota, R. Fukuda, J. Hasegawa, M. Ishida, T. Nakajima, Y. Honda, O. Kitao, H. Nakai, T. Vreven, J.A. Montgomery Jr., J.E. Peralta, F. Ogliaro, M. Bearpark, J.J. Heyd, E. Brothers, K.N. Kudin, V.N. Staroverov, R. Kobayashi, J. Normand, K. Raghavachari, A. Rendell, J.C. Burant, S.S. Iyengar, J. Tomasi, M. Cossi, N. Rega, J.M. Millam, M. Klene, J.E. Knox, J.B. Cross, V. Bakken, C. Adamo, J. Jaramillo, R. Gomperts, R.E. Stratmann, O. Yazyev, A.J. Austin, R. Cammi, C. Pomelli, J.W. Ochterski, R.L. Martin, K. Morokuma, V.G. Zakrzewski, G.A. Voth, P. Salvador, J.J. Dannenberg, S. Dapprich, A.D. Daniels, O. Farkas, J.B. Foresman, J.V. Ortiz, J. Cioslowski, D.J. Fox, Gaussian 09, Revision A.1, Gaussian, Inc., Wallingford, CT, 2009.
[30] J.P. Perdew, K. Burke, M. Ernzerhof, Generalized gradient approximation made simple, Phys. Rev. Lett. 77 (1996) 3865–3868.
[31] J.P. Perdew, K. Burke, M. Ernzerhof, Generalized gradient approximation made simple, Phys. Rev. Lett. 78 (1997) 1396.
[32] J.S. Gancheff, P.A. Denis, Time-dependent density functional theory investigation of the electronic spectra of hexanuclear chalcohalide rhenium(III) clusters, J. Phys. Chem. A 115 (2011) 211–218.
[33] V.N. Nemykin, R.G. Hadt, R.V. Belosludov, H. Mizuseki, Y. Kawazoe, Influence of molecular geometry exchange-correlation functional, and solvent effects in the modeling of vertical excitation energies in phthalocyanines using time-dependent density functional theory (TDDFT) and polarized continuum model TDDFT methods: can modern computational chemistry methods explain experimental controversies? J. Phys. Chem. A 111 (2007) 12901–12913.
[34] B. Champagne, M. Guillaume, F. Zutterman, TD-DFT investigation of the optical properties of cyanine dyes, Chem. Phys. Lett. 425 (2006) 105–109.
[35] B. Champagne, E. Botek, O. Quinet, M. Nakano, R. Kishi, T. Nitta, K. Yamaguchi, Polarizability and second hyperpolarizability of open-shell π-conjugated compounds from spin projection method calculations, Chem. Phys. Lett. 407 (2005) 372–378.
[36] S. Hirata, M. Head-Gordon, Time-dependent density functional theory for radicals. An improved description of excited states with substantial double excitation character, Chem. Phys. Lett. 302 (1999) 375–382.
[37] A. Spielfiedel, N.C. Handy, Potential energy curves for PO, calculated using DFT and MRCI methodology, Phys. Chem. Chem. Phys. 1 (1999) 2401–2409.
[38] Y.Q. Qiu, H.L. Fan, S.L. Sun, C.G. Liu, Z.M. Su, Theoretical study on the relationship between spin multiplicity effects and nonlinear optical properties of the pyrrole radical (C4H 4N), J. Phys. Chem. A 112 (2008) 83–88.
[39] V.N. Nemykin, P. Basu, Comparative theoretical investigation of the vertical excitation energies and the electronic structure of $[MoVOCl_4]^-$: Influence of basis set and geometry, Inorg. Chem. 42 (2003) 4046–4056.
[40] J. Preat, D. Jacquemin, V. Wathelet, J.-M. André, E.A. Perpète, TD-DFT investigation of the UV spectra of pyranone derivatives, J. Phys. Chem. A 110 (2006) 8144–8150.
[41] A. Trujillo, M. Fuentealba, D. Carrillo, C. Manzur, I. Ledoux-Rak, J.-R. Hamon, J.-Y. Saillard, Synthesis, spectral, structural second-order nonlinear optical properties and theoretical studies on new organometallic donor–acceptor substituted nickel(II) and copper(II) unsymmetrical Schiff-base complexes, Inorg. Chem. 49 (2010) 2750–2764.
[42] C. Dehu, F. Meyers, J.L. Bredas, Donor–acceptor diphenylacetylenes: geometric structure, electronic structure, and second-order nonlinear optical properties, J. Am. Chem. Soc. 115 (1993) 6198–6206.
[43] F. Sim, S. Chin, M. Dupuis, J.E. Rice, Electron correlation effects in hyperpolarizabilities of *p*-nitroaniline, J. Phys. Chem. 97 (1993) 1158–1163.
[44] H. Sekino, Y. Maeda, M. Kamiya, K. Hirao, Polarizability and second hyperpolarizability evaluation of long molecules by the density functional theory with long-range correction, J. Chem. Phys. 126 (2007) 014107 (1–6).
[45] D. Jacquemin, E.A. Perpète, M. Medved, G. Scalmani, M.J. Frisch, R. Kobayashi, C. Adamo, First hyperpolarizability of polymethineimine with long-range corrected functionals, J. Chem. Phys. 126 (2007) 191108 (1–4).
[46] C. Adamo, V. Barone, Toward reliable density functional methods without adjustable parameters: the PBE0 model, J. Chem. Phys. 110 (1999) 6158–6170.
[47] C. Adamo, V. Barone, Accurate excitation energies from time-dependent density functional theory: assessing the PBE0 model for organic free radicals, Chem. Phys. Lett. 314 (1999) 152–157.
[48] D.A. Kleinman, Nonlinear dielectric polarization in optical media, Phys. Rev. 126 (1962) 1977–1979.
[49] S.D. Cummings, L.-T. Cheng, R. Eisenberg, Metalloorganic compounds for nonlinear optics: molecular hyperpolarizabilities of M(diimine)(dithiolate)complexes (M = Pt, Pd Ni), Chem. Mater. 9 (1997) 440–450.
[50] J.L. Oudar, Optical nonlinearities of conjugated molecules Stilbene derivatives and highly polar aromatic compounds, J. Chem. Phys. 67 (1977) 446–457.
[51] J.L. Oudar, D.S. Chemla, Hyperpolarizabilities of the nitroanilines and their relations to the excited state dipole moment, J. Chem. Phys. 66 (1976) 2664–2668.